A Josephson relation for fractionally charged anyons.

M. Kapfer[1], P. Roulleau[1], I. Farrer[2,3], D.A. Ritchie[2], & D. C. Glattli[1]

[1]Service de Physique de l'Etat Condensé, IRAMIS/DRF (CNRS UMR 3680), CEA Saclay, F-91191 Gif-sur-Yvette, France.

[2] Cavendish Laboratory, University of Cambridge, J.J. Thomson Avenue, Cambridge CB3 0HE, UK.

[3] Department of Electronic and Electrical Engineering, University of Sheffield, Mappin Street, S1 3JD, UK.

In some quantum matter states, the electrical current may remarkably be transported by carriers bearing a fraction e* of the elementary charge e. This is the case for the topological ordered states of the fractional Quantum Hall Effect (FQHE)[1,2] which occurs in two-dimensional electron systems in high magnetic field. When the magnetic flux per electron, in units of the quantum flux h/e, is a fraction ν=p/q, a dissipationless current carried by anyons with fractional charge[2] e*=e/q flows around the sample edges. Among the early attempts to observe these fractional charges[3-8], the most reliable ones[4-8] were based on measuring the tiny current noise[9-11], or shot noise, that produces their granularity. Here we report on dynamical properties of anyons. We measure, for charge e*=e/3 and e/5, the long predicted Josephson frequency $f_J = e^*V/h$[11-12]. It manifests as marked signatures in the Photo Assisted Shot Noise (PASN) versus voltage V when irradiating contacts with microwaves at frequency $f=f_J$[13-15]. The Josephson relation provides a novel accurate determination of anyon charges. Importantly, its observation validates FQHE PASN[13-15] models enabling time-domain manipulations of anyons and the realization of on-demand single anyon sources based on levitons[16,17,14,18] to perform Hong Ou Mandel tests[17,19] of their anyonic statistics[20].

The Quantum Hall Effect (QHE) occurs in two-dimensional electron systems (2DES) for strong magnetic fields quantizing the electron cyclotron energy into Landau levels. For integer Landau level filling factor ν=p, the Integer QHE (IQHE) shows a

topologically protected quantized Hall conductance pe^2/h with zero longitudinal conductance[21]. For very low disorder samples, the Coulomb repulsion favors topologically ordered phases at rational $\nu=p/q$ showing a Fractional QHE (FQHE) with fractional Hall[1] and zero longitudinal conductance. For electrons filling the first Landau Level ($\nu<1$), the states with $\nu=1/(2k+1)$ are well understood by Laughlin states[2]. The elementary excitations, or quasiparticles, bear a fraction $e^*=e/(2k+1)$ of the elementary charge and are believed to obey a fractional anyonic[20] statistics intermediate between bosons and fermions. For $\nu<1$, the Jain states with $\nu=p/(2kp+1)$, p and k integer, display $e^*=e/(2kp+1)$ fractionally charged excitations which are composite fermions, i.e., electrons to which –2k flux quanta $\phi_0=h/e$ are attached[22]. For higher Landau Level filling, even denominators FQHE states are found such as the 5/2 state showing Majorana excitations and $e^*=e/4$ non-abelian anyonic quasiparticles[23]. The FQHE is the first example of topological matter hosting fractional excitations with possibly fractional statistics and its understanding is of utmost importance. An important breakthrough would be the time domain manipulation of the fractional excitations. Combining microwave frequency irradiation with low frequency shot noise measurements, this work provides an experimental test of our understanding of the dynamics of fractional excitations by validating PASN models. By demonstrating a novel dynamical property of anyons and measuring their Josephson frequency $f_J= e^*V/h$, we provide a direct comparison of voltage to frequency giving a fundamental determination of the anyon charge.

The concept of the fractional Josephson frequency in the FQHE regime first appeared in the theory work of X. G. Wen and collaborators who considered photo-assisted processes[12] or finite frequency noise[11] and it was later used in PASN models[13-15,18]. The Josephson frequency has a long history starting from the discovery of the AC Josephson Effects[24,25] in superconductors. When two tunnel coupled superconductors are biased by a voltage V_{dc}, a steady current oscillation occurs at frequency f_J providing evidence of the Cooper pair charge $e^*=2e$. An inverse AC Josephson effect occurs when irradiating the superconducting junction at frequency f, giving photon-assisted singularities in the I-V characteristics, the so-called Shapiro steps[25], when the bias voltage Josephson frequency f_J matches a multiple of f.

Fundamentally, the AC Josephson effects arise from the quantum beating between tunnel coupled Cooper pairs in the condensate at energies separated by eV_{dc}. For normal metals, described by a Fermi sea, no steady Josephson oscillations are expected but transient current oscillations at frequency $f_J=eV_{dc}/h$ were recently demonstrated in numerical quantum simulations for two voltage shifted Fermi seas put in quantum superposition in an electronic interferometer[26]. Also in normal metals, the Josephson frequency manifests itself in the high frequency shot noise when the bias voltage equals the emission noise frequency. Reciprocally, the low frequency photo-assisted shot noise (PASN) shows Josephson like singularities when microwaves irradiate a contact at frequency $f=f_J$. In the following, we will focus on PASN.

First predicted[27] for mesoscopic normal conductors, PASN is expected to occur in all electronic systems, even interacting ones like the FQHE, providing means to determine e* from the Josephson frequency[13-15]. In absence of microwave irradiation the (DC) shot noise is the result of the quantum beating of two voltage shifted Fermi seas when scattering in the conductor mixes the carrier states. For a single mode normal conductor (e*=e) with conductance $g_0=e^2/h$ and a unique scatterer of reflection probability R, the zero temperature current noise spectral density under DC bias V_{dc} is given by $S_I^{DC} = 2g_0 R(1-R)e|V_{dc}|$. When adding an AC voltage to the biased contact: $V(t)=V_{dc} + V_{ac}\cos(2\pi ft)$, the phase of all carriers emitted by the contact gets a time dependent part $\phi(t) = \frac{e^*}{h}\int_{-\infty}^{t} V(t')dt'$ giving rise to energy scattering. The emitted carriers end in a superposition of quantum states with energy shifted by lhf and probability amplitude $p_l = \frac{1}{2\pi}\int_0^{2\pi} e^{-i\phi(t)} e^{i2\pi l f t} dt$, l integer. Using the voltage V_{dc} in units of the Josephson frequency $f_J=e^*V_{dc}/h$, the predicted PASN spectral density can be written as:

$$S_I^{PASN}(f_J) = \sum_{l=-\infty}^{l=\infty} |p_l|^2 S_I^{DC}(f_J - lf) \qquad (1)$$

where S_I^{DC} is the DC shot noise measured when V_{ac}=0. Eq.(1) expresses that the measured observable is the result of the sum of simultaneous measurements with shifted voltage $V_{dc} \rightarrow V_{dc}+lhf/e^*$ and weighted by the probability $|p_l|^2$, as the Fermi sea of the driven contact is in a quantum superposition of states with energy shifted by *lhf*. Interestingly the zero bias voltage DC shot noise singularity, $\sim|V_{dc}|\sim|f_J|$, is replicated whenever $f_J = e^*V_{dc}/h = lf$, signalling the Josephson frequency. Although less spectacular, this effect parallels in the noise the Shapiro steps of superconducting junctions IVC, i.e. the inverse AC Josephson effect[25]. The observation of the PASN singularity for $f_J=eV_{dc}/h=f$ is well documented in normal conductors[28,30,31] (e*=e), like diffusive metallic wires[28], Quantum Point Contacts[30], and tunnel junctions[31]. Regarding interactions, (1) has been tested in superconducting/normal junctions (e*=2e)[29]. For the FQHE, expression (1) was explicitly shown in[14] and is implicit in PASN expressions of refs[13,15,19]. No experiment has been reported since the combination of high magnetic fields, sub-fA/Hz$^{1/2}$ current noise and >10 GHz microwaves at ultra-low temperature (~20mK) is highly demanding.

The present work fills this gap. A schematic view of the set-up and the sample is shown in Fig.1(a). In topologically insulating QHE conductors the current flows along chiral edge modes. There are p chiral modes for filling factor $\nu=p/(2p+1)$. To inject current or apply a microwave excitation, metallic contacts connect the edges to an external circuit. A narrow tuneable constriction called Quantum Point Contact (QPC) is formed by applying a negative voltage V_G to split gates to induce quantum scattering by mixing counter-propagating edge modes. Carriers incoming from contact 0 and scattered by the QPC contribute to transmitted and backscattered currents, I_t and I_B respectively. They are measured at contact (1,2) via the voltages $V_{1(2)}=(h/e^2\nu_B)I_{t(B)}$ where ν_B is the filling factor in the lead (far from the QPC). The partitioning of the carrier generates a current noise S_I which is measured by recording the negative cross-correlation of the voltage fluctuations $\Delta V_{1(2)}=(h/e^2\nu_B)\Delta I_{t(B)}$ giving $S_I = -\langle \Delta I_t \Delta I_B \rangle / \Delta f$. Δf is the bandwidth of the low frequency resonant detecting circuit (see method).

We concentrate our study on bulk filling factor ν_B =2/5 which allows us to conveniently probe e/3 or e/5 excitations. The two co-propagating chiral edge modes of the 2/5 Jain state are revealed by sweeping the QPC gate voltage V_G as shown in Fig.1(b). Starting with a $(2/5)e^2/h$ conductance plateau we observe a second conductance plateau $(1/3)e^2/h$ at lower V_G. This corresponds to a fully reflected inner channel with conductance $g_2=(2/5-1/3)e^2/h$ while the outer edge channel with conductance $g_1=(1/3)e^2/h$ is fully transmitted. To probe the e/3 charged excitations of the 1/3-FQHE state locally formed at the QPC, V_G is set to -0.090V (point (A) in Fig.1(b)) so as to induce a weak backscattering (WB) between counter-propagating outer edge modes with reflection probability R=0.026 . The transmitted and backscattered conductances of the outer edge channel are $G_t=(1-R)g_1$ and $G_B= Rg_1$ respectively. Next, we apply a dc voltage V_{dc} to the injecting contact. The incoming current of the outer edge mode $I_0=(1/3)(e^2/h)V_{dc}$ divides into a backscattering current $I_B \approx RI_0$ and a forward current $I=I_0-I_B$. In the FQHE, the chiral modes form chiral Luttinger liquids and the transport properties at finite backscattering become energy dependent. This gives non-linear variations of the backscattered current I_B with voltage V_{dc}. A complete modelling is difficult and comparison to experiments is only easy in the WB regime (R<<1). The small backscattered current $I_B(V_{dc})$ results from rare quasiparticle tunnelling events which follow Poissonian statistics. In this limit, the DC shot noise current noise cross-correlation is given by[11-13]

$$S_I^{dc}(V_{dc}) = 2e^* I_B(V_{dc})[\coth(e^*V / 2k_BT_e) - 2k_BT_e / e^*V_{dc}] \qquad (2)$$

with e*=e/3 for the 1/3-FQHE regime considered here and T_e the electronic temperature.

Fig. 2(b), black dots, shows DC shot noise data. The black dashed line, computed using Eq.(2) compares well with the data for e*=e/3. Here a constant R≈0.026 versus V_{dc} is used as $I_B(V_{dc})$ is found to be almost linear (see Supplementary Information S.I., Fig.S3).

Next, to show the Josephson relation using PASN, the AC voltage $V_{ac}(t)=V_{ac}\cos 2\pi ft$ is superimposed on V_{dc} with f=22GHz. The blue and red dots show

the measured (PASN) noise for several V_{ac} corresponding to -61 and -67dBm nominal RF power (disregarding rf lines losses) sent to the contact. At low V_{dc}, the PASN noise increases with power and merges into the DC shot noise curve for V_{dc} above ≈250μV. In order to reveal the pure photon-assisted contribution to PASN, guided by the form of Eq.(1), we subtract the independently measured DC shot noise data from the raw PASN data to obtain the Excess PASN defined as $\Delta S_I = S_I^{PASN}(V_{dc}) - |p_O|^2 S_I^{dc}(V_{dc})$. Finding the condition to cancel the DC shot noise term in ΔS_I provides the value of $|p_0|^2=J_0(\alpha)^2$ for the excitation $V_{ac}=\alpha hf/e^*$ used. This is done for three RF powers: 67, 63, and 61dBm (see S.I., Fig.S4). To improve the data statistics, the average of the three excess PASN curves is calculated and shown in Fig.2(c), blue dots. Neglecting $|l|>1$ photon process and using the average $|p_1|^2$ values obtained from the average $|p_0|^2$ value: $\langle|p_1|^2\rangle=(1-\langle|p_0|^2\rangle)/2$ the theoretical Excess PASN is:

$$\Delta S_I(f_J^*) = \left\langle |p_1|^2 \right\rangle S_I^{DC}(f_J - f) + \left\langle |p_1|^2 \right\rangle S_I^{DC}(f_J + f) \qquad (3)$$

Eq(3) is plotted using $f_J=(e/3)V_{dc}/h$ as a blue dashed line in Fig.2(c). It is remarkable that the extracted value of $\langle|p_1|^2\rangle$ and the choice of f_J accounts well for the actual Excess PASN variation observed. This strongly supports the validity of Eq.(1).

A further validation of (1) is given by changing the excitation frequency. We have repeated similar measurements and analyses for f=17GHz and f=10GHz. In Fig.2(c), the green and red dot curves show excess PASN data and the green and red dashed line provide a convincing comparison to Eq.(3). Within thermal rounding effects $\approx k_B T_e/e^*$ the voltage V_J signalling the onset of excess PASN gives the Josephson frequency which matches the excitation frequency. $V_J= hf/e^*$, with e* a free parameter, is extracted from best fit of Eq.(3) to the excess PASN data for each frequency f. Then V_J is plotted in Josephson frequency units $(e/3)V_J/h$ versus f in Fig.2(d). The straight line, slope one, corresponds to $e^*=e/3$ exactly. A linear fit of the data gives $e^*=e/(3.07 \pm 0.05)$.

Finally we confirm that we are measuring the Josephson frequency by changing the excitation charge. We now consider the WB regime of the inner edge of the 2/5 FQHE Jain state, associated with the conductance $(2/5-1/3)e^2/h$, see Fig.3(a).

The backscattered current is now $I_B=R(1/15)e^2/hV_{dc}$. We set V_G to -0.03V for which R=0.064, point (B) of Fig.1(b). Fig. 3(b) shows the DC noise data (black dots). A comparison of data using Eq.(2) with e*=e/5 and R=0.064 (black dashed lines) confirms a one-fifth quasiparticle charge as in[6]. The PASN for various RF power at 17 GHz is shown as coloured circles. As previously done for e/3 charges, we average the PASN data at 17GHz for three different Rf power (-60, -58 and -55dBm). The resulting mean excess noise $\langle \Delta S_I \rangle = \left\langle S_I^{PASN}(V_{dc}) \right\rangle - \left\langle |p_O|^2 \right\rangle S_I^{dc}(V_{dc})$ is plotted in Fig.3(c) (blue dots). The data compare well with the computation of Eq.(3) (red dashed line), using $f_J=(e/5)V_{dc}/h$ and $\langle|p_1|^2\rangle=(1-\langle|p_0|^2\rangle)/2$, including a finite temperature T_e=30mK. A similar procedure is done for 10GHz excitation. Then, the voltage $V_J=hf/e^*$ characterising the onset of excess PASN is left as a free parameter to fit the excess PASN data and is plotted in units of Josephson frequency $f_J=(e/5)V_J/h$ versus f, in Fig.3(d). The dashed line, slope one, corresponds to e*=e/5 exactly. A linear fit of the actual V_J versus f passing by zero gives e*=e/(5.17±0.31).

Similar measurements have been repeated for the WB regime at ν_B=1/3 and 2/3, confirming Josephson frequency with charge e/3. This will be published in a longer paper. Future experiments will measure f_J for non-abelian anyons at ν_B=5/2 in ultra-high mobility samples. This will be important as the direct comparison of voltage to frequency is metrological and free of unknown parameters. Another perspective is the realization of a single charge source based on levitons using periodic Lorentzian voltage pulses instead of a sine wave. The PASN due to periodic levitons is also given by Eq.(1) except that all the p_l for l<0 vanish, characterizing a minimal excitation state without hole-like excitations[17], see S.I. . A charge e Leviton sent to a QPC in the WB regime would provide a convenient time controlled single anyon source with Poisson's statistics[14,18]. Combining two similar sources opens the way for Hong Ou Mandel anyon interference to probe the anyonic statistics[19].

Method :

Sample characteristics and fabrication: samples are 2DES with electrons confined at the interface of high mobility epitaxial grown GaAs/GaAlAs heterojunctions at 90 nm below the surface. The low temperature zero field mobility is 2

$10^6 cm^2 s^{-1} V^{-1}$ and the electron density is n_s=1,11 $10^{15} m^{-2}$. For this density, the bulk filling factor ν_B=2/5 corresponds to a magnetic field of 11.2 Tesla. Ohmic contacts are realized by evaporating 125 nm Au, 60 nm Ge, 4 nm Ni followed by annealing at 470°C. A shallow mesa etching (H3PO4 phosphoric acid, time 4 minutes) defines the sample. The QPC gates are realized by e-beam lithography, see SI, Fig.S1 for a SEM image of the sample used.

Measurement set-up: an ultra-low temperature cryo-free dilution refrigerator with a 22 mK base temperature from CryoConcept is used. It is equipped with a dry superconducting coil able to reach 14.5 Tesla. Ultra-low-loss dc-40GHz microwave cables, same as in ref.[17], bring the room temperature microwave excitation from an Agilent N5183A RF source to a PCB. The nominal RF power given in the main text is estimated from the RF source power and the fixed 60dB cold attenuators. A nominal -60dBm rf power corresponds to $V_{ac}^{nom} \approx 450$ μV. However the actual V_{ac} can be smaller due to extra losses in the coaxial lines. Dynamical screening in the FQHE sample may also affects V_{ac}. Coplanar waveguides designed by CST microwave Studio^R etched on the PCB bring the radiofrequency to the ohmic contact (0) of the sample, see Fig.1(a) and S1. Noise measurements are obtained by separately converting the transmitted and reflected current fluctuations into voltage fluctuations at contact (1) and (2) respectively in parallel to a R-L-C resonant circuit tuned to 2,5 MHz frequency and bandwidth 700 kHz, with R=20kOhms. The voltage fluctuations are amplified by two home-made cryogenic amplifiers with 0.22 $nV/Hz^{1/2}$ input noise at low temperature, followed by low noise room temperature amplifiers. The amplified fluctuations are passed through Chebyshev filters and then sent to a fast 20Ms/s digital acquisition card (ADLink 9826) while a PC provides real-time computation of the cross-correlation spectrum. Absolute Noise calibration is done by recording the equilibrium Johnson Nyquist noise when varying the temperature from 20mK to 200mK. Differential Conductance measurements giving the transmission and reflection are made by applying a low 0,7 kHz frequency sub-μV amplitude voltage to contact (0) and sending the amplified AC voltage from contacts (1) and (2) to two Lock-in amplifiers. The measurement accuracy is mostly limited by the large 1/f noise of the cryogenic HEMT. The shot noise accuracy is limited by the input white noise

of the amplifier and time averaging. For ν_B=2/5, the 20kOhm resistor and the ≈5kOhm Inductance parallel resistance in parallel with the bulk Hall resistance converts the input noise of 220pV/Hz$^{1/2}$ into 210^{-27}A^2/Hz equivalent current noise power. Using cross-correlation and noise averaging during the measurement time τ=300s with ≈350kHz effective detection bandwidth, the accuracy of a raw noise data point is ~3 10^{-31}A^2/Hz.

Data analysis: In the IQHE regime the finite temperature expression for cross-correlated shot noise of a single channel is:

$$S_I^{dc}(V_{dc}) = 2eR(1-R)\frac{e^2}{h}V_{dc}(\coth(eV_{dc}/2k_BT_e) - 2k_BT_e/eV_{dc}) \qquad (4)$$

where R is the reflection coefficient and T_e the electronic temperature. In the FQHE regime, for very weak reflection coefficient, the backscattering current $I_B(V_{dc})$ is almost linear with voltage, see Fig.S2(a) and S3 in S.I., and one can use the following expression :

$$S_I^{dc}(V_{dc}) = 2e^*R(1-R)gV_{dc}(\coth(e^*V_{dc}/2k_BT_e) - 2k_BT_e/e^*V_{dc}) \qquad (5)$$

(5) is identical to (2) but written differently, g being the conductance of the open fractional channel considered. To find the excess PASN ΔS_I given by Eq.(3) we subtract the appropriate amount of DC shot noise by controlling the weighted $|p_0|^2$ so as to obtain a constant noise at low bias voltage in the range $|V_{dc}|<hf/e$. This provides a measure of $|p_0|^2=J_0(\alpha)^2$. We then observe that the noise is flat over a larger voltage scale given by $|V_{dc}|<(hf-k_BT_e)/e^*$. However there is a small T_e increase, several tens of mK, due to RF heating and subtracting the DC shot noise at the lowest temperature prevents a perfect cancellation of noise variation at small bias over the range $|V_{dc}|<k_BT_e/e^*$. We then subtract from the PASN data the DC shot noise given by (5) and adjust T_e for the best noise variation cancellation over the full range $|V_{dc}|<hf/e$. We note that only the form of PASN given by Eq.(1), with a discrete sum of shifted voltages, can lead to a flat noise variation. If the PASN was given by a trivial classical time averaging of the noise $<S_I^{DC}(V(t))>$ with $V(t)=V_{dc}+V_{ac}\cos(2\pi ft)$, such cancellation would be impossible, see Fig.S7 in S.I. . Importantly, the low voltage bias

constant noise signalling the cancellation of the DC shot noise, occurs because the noise is symmetric and linear with respect to bias voltage V_{dc}.

Data availability

The data that support the findings of this study are available from the corresponding author on reasonable request.

References

1. D.C. Tsui, H.L. Stormer, A.C. Gossard, Two-Dimensional Magnetotransport in the Extreme Quantum Limit. *Phys. Rev. Lett.* **48**, 1559 (1982)
2. Laughlin R. B., Anomalous Quantum Hall Effect: An Incompressible Quantum Fluid with Fractionally Charged Excitations. *Phys. Rev. Lett.* **50**, 1395 (1983)
3. Goldman, V. J. & Su, B. Resonant tunneling in the fractional quantum Hall regime: measurement of fractional charge. *Science* **267**, 1010–1012 (1995)
4. Saminadayar L., Glattli D. C., Jin Y., and Etienne B., Observation of the e/3 Fractionally Charged Laughlin Quasiparticle. *Phys. Rev. Lett.* **79**, 2526 (1997)
5. de-Picciotto R, et al. Direct observation of a fractional charge. *Nature* **389**,162-164 (1997)
6. Reznikov M, De Picciotto R, Griffiths TG, Heiblum M, Umansky V Observation of quasiparticles with one-fifth of an electron's charge. *Nature* 3**99**, 238–241 (1999)
7. M. Dolev, M. Heiblum, V. Umansky, Ady Stern, and D. Mahalu Observation of a quarter of an electron charge at the ν= 5/2 quantum Hall state. *Nature* **452**, 829 (2008)

8. Hashisaka M., Ota T., Muraki K., and Fujisawa T., Shot-Noise Evidence of Fractional Quasiparticle Creation in a Local Fractional Quantum Hall State. *Phys. Rev. Lett.* **114**, 056802 (2015).

9. Kane, C. L. & Fisher, M. P. A. Nonequilibrium noise and fractional charge in the quantum Hall effect. *Phys. Rev. Lett.* **72**, 724–727 (1994).

10. Fendley, A., Ludwig, W. W. & Saleur, H. Exact nonequilibrium DC shot noise in Luttinger liquids and fractional quantum Hall devices. *Phys. Rev. Lett.* **75**, 2196-2199 (1995)

11. de Chamon, C., Freed, D. E. & Wen, X. G. Tunneling and quantum shot noise in Luttinger liquids. *Phys. Rev. B* **51**, 2363–2378 (1995).

12. Wen, X. G. Edge transport properties of the fractional quantum Hall states and weak-impurity scattering of a one-dimensional charge-density wave. *Phys. Rev. B* **44**, 5708 (1991)

13. Crépieux A., Devillard P., Martin T., Photoassisted current and shot noise in the fractional quantum Hall effect. *Phys. Rev. B* **69**, 205302 (2004)

14. Safi I. Time-dependent Transport in arbitrary extended driven tunnel junctions. arXiv:1401.5950 [cond-mat.mes-hall] (2014)

15. Chevallier D. , Jonckheere T. , Paladino E. , Falci G. , and Martin T., Detection of finite-frequency photoassisted shot noise with a resonant circuit. *Phys. Rev. B* **81**, 205411 (2010)

16. Levitov, L. S., Lee, H. & Lesovik, G. Electron counting statistics and coherent states of electric current. *J. Math. Phys.* **37**, 4845–4886 (1996)

17. Dubois, J. Jullien, T., Portier, F., Roche, P., Cavanna, A., Jin, Y., Wegscheider, W., Roulleau, P., and Glattli, D.,C., Minimal-excitation states for electron quantum optics using levitons. *Nature* **502**, 659–663 (2013)

18. Rech J., Ferraro D., Jonckheere T., Vannucci L., Sassetti M., and Martin T. , Minimal Excitations in the Fractional Quantum Hall Regime. *Phys. Rev. Lett.* **118**, 076801 (2017)

19. Bäuerle C., Glattli D. C., Meunier T., Portier F., Roche P., Roulleau P., Takada S., and Waintal X., Coherent control of single electrons: a review of current progress. *Rep. Prog. Phys.* **81** (2018) 056503 (33pp)

20. Arovas D., Schrieffer J. R., and Wilczek F., Fractional Statistics and the Quantum Hall Effect. *Phys. Rev. Lett.* **53**, 722 (1984)

21. Klitzing K. v., Dorda G., and Pepper M., New Method for High-Accuracy Determination of the Fine-Structure Constant Based on Quantized Hall Resistance. *Phys. Rev. Lett.* **45**, 494 (1980).

22. Jain J. K. Composite-fermion approach for the fractional quantum Hall effect. *Phys. Rev. Lett.* **63**, 199 (1989)

23. Moore, G. & Read, N. Nonabelions in the fractional quantum Hall effect. *Nucl. Phys. B* **360**, 362–396 (1991)

24. Josephson B. D., Possible new effects in superconductive tunnelling. *Phys. Lett.*, **1**, 251 (1962).

25. Shapiro S., Josephson Currents in Superconducting Tunneling: The Effect of Microwaves and Other Observations. *Phys. Rev. Lett.* **11**, 80 (1963)

26. Gaury B., Weston J., and Waintal X., The a.c. Josephson effect without superconductivity. *Nature Comm.* **6**, 6524 (2015)

27. Lesovik G. B. and Levitov L. S., Noise in an ac biased junction: Nonstationary Aharonov-Bohm effect. *Phys. Rev. Lett.* **72**, 538 (1994)

28. Schoelkopf R., Kozhevnikov A., Prober D., and Rooks M. Observation of "Photon-Assisted" Shot Noise in a Phase-Coherent Conductor. *Phys. Rev. Lett.* **80**, 2437 (1998)

29. Kozhevnikov A. A. , Schoelkopf R. J. , and Prober D. E. Observation of Photon-Assisted Noise in a Diffusive Normal Metal–Superconductor Junction. *Phys. Rev. Lett.* **84**, 3398 (2000)

30. Reydellet L.-H. , Roche P., Glattli D. C., Etienne B., and Jin Y. Quantum Partition Noise of Photon-Created Electron-Hole Pairs. *Phys. Rev. Lett.* **90**, 176803 (2003)

31. Gabriel Gasse G., Spietz L., Lupien C., and Reulet B., Observation of quantum oscillations in the photoassisted shot noise of a tunnel junction. *Phys. Rev. B* **88**, 241402(R) (2013).

Figure Legends:

Figure 1: experiment schematics for PASN measurements.

(a) Experiment principle: a DC voltage V_{dc} is applied to contact (0) which injects carriers at bulk filling factor $\nu_B=2/5$ into two chiral fractional edge modes (red lines). The carrier are partitioned by a quantum point contact (QPC) into transmitted and reflected current which are absorbed at the grounded contacts giving rise to the Hall voltages $V_t = I_t h/\nu_B e^2$ and $V_B = I_B h/\nu_B e^2$ at contact (1) and (2). The negative voltage fluctuations cross-correlations $\Delta V_t \Delta V_B = -(h/\nu_B e^2)^2 S_I \Delta f$ are recorded to obtain the current noise S_I. This is done by sending the voltages to two identical resonant circuits followed by cryogenic amplifiers whose output is send to a fast acquisition card. A computer performs the FFT cross-correlation(see Methods). The RF excitation coming from the microwave photon source is added to V_{dc} with a Bias Tee and sent to contact (0).

(b) Fractional conductance and working points. The figure shows the transmitted conductance $G_t=dI_t/dV_{dc}$ at bulk filling factor $\nu_B=2/5$ versus the QPC gate voltage. The $(2/5)e^2/h$ plateau is followed by a $(1/3)e^2/h$ plateau signaling complete reflection of the inner 2/5 fractional edge channel. Points

(A) and (B) show the weak backscattering conditions for measurements with fractional carrier e/3 and e/5 respectively.

Figure 2: Josephson relation for 1/3 FQHE state.

(a) Chiral edge schematics: the fully reflected 2/5 inner edge state gives rise to a ν=1/3 FQHE state at the QPC. For V_G=-0.090V, point (A) of Fig.1(b), the counter-propagating outer edges state are weakly coupled, allowing to probe e/3 backscattered carriers.

(b) Raw shot noise measurements: Black dots show the DC shot noise (i.e. with only V_{dc} applied at contact (0) and no RF). The dashed line is Eq.(2) with e*=e/3 and constant R=0.026 (point (A) of Fig.1(a)). Blue and red open circles are noise measurements for 22GHz -67dBm and -61dBm RF irradiation. Blue and red dashed line curve are comparison using Eq. (1) with $f_J=(e/3)V_{dc}/h$ (see Supplementary Information).

(c) Excess PASN ΔS_I (blue, green and red dots) for three frequencies 22, 17 and 10GHz respectively. The average of measurements at several excitation power is shown to improve the noise statistics. The blue, green and red dashed lines, computed from Eq.(3) using $f_J=(e/3)V_{dc}/h$, compare well to the data. For clarity the constant $\Delta S_I(V_{dc}= 0)$ has been subtracted from the excess PASN and the 17 and 10 GHz data have been offset.

(d) Determination of carrier charge from the Josephson relation. A best fit of ΔS_I gives, for each frequency, the threshold voltages $V_J=hf/e^*$ above which ΔS_I rises. They are plotted in units of $(e/3)V_J/h$ versus f. The dashed line

corresponds to $e^*=e/3$ exactly. According to uncertainties, one finds $e^*=e/(3.06 \pm 0.20)$.

Figure 3: Josephson relation for the 2/5 FQHE state.

(a) Chiral edge schematics: the 2/5 inner edge state is weakly reflected, see point (B) of Fig.1(b). Here backscattered $e^*=e/5$ carriers contribute to current I_B and shot noise S_I.

(b) Raw shot noise measurements: Black dots shows the DC shot noise (i.e. no RF) measured during the 17GHz PASN measurement run. The black dashed line is Eq.(2) using R=0.064 (point (B) of Fig.1(a)). Blue and red open circles is the PASN for 17GHz -58dBm and -51dBm RF irradiation. Blue and red dashed line curve are comparison using Eq (1) with $f_J=(e/5)V_{dc}/h$ (see Supplementary Information).

(c) Excess PASN ΔS_I. Green and red dots correspond to 17 and 10 GHz. Green and red dashed lines are computed from Eq.(3) using $f_J=(e/5)V_{dc}/h$. For clarity $\Delta S_I(V_{dc}=0)$ has been subtracted from the excess PASN.

(d) Determination of e^*: a best fit of ΔS_I gives, for each frequency, the threshold voltages $V_J=hf/e^*$ above which ΔS_I rises. They are plotted in units of $(e/5)V_J/h$ versus f. The dashed line corresponds to $e^*=e/5$ exactly. According to uncertainties, one finds $e^*=e/(5.17 \pm 0.31)$.

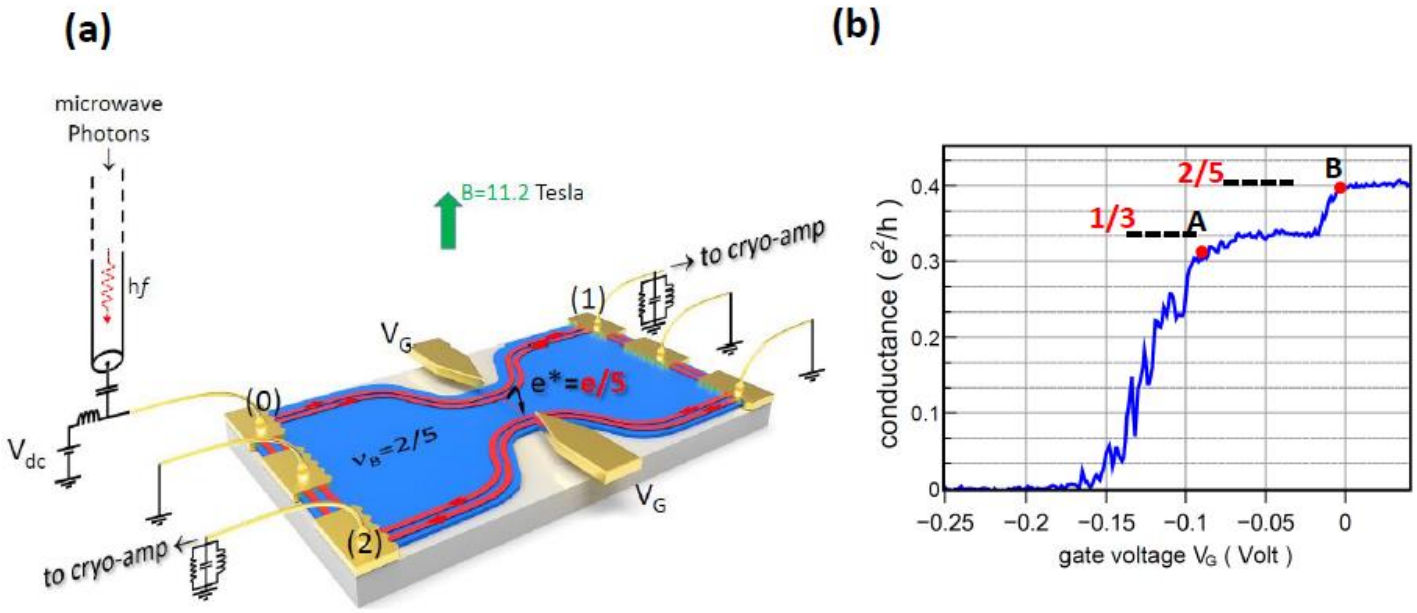
(a)
(b)
microwave
Photons
hf
B=11.2 Tesla
to cryo-amp
(1)
V_G
e*=e/5
(0)
V_{dc}
ν_B=2/5
V_G
to cryo-amp
(2)
2/5
B
1/3
A
conductance (e^2/h)
0.4
0.3
0.2
0.1
0
−0.25
−0.2
−0.15
−0.1
−0.05
0
gate voltage V_G (Volt)

Figure 1

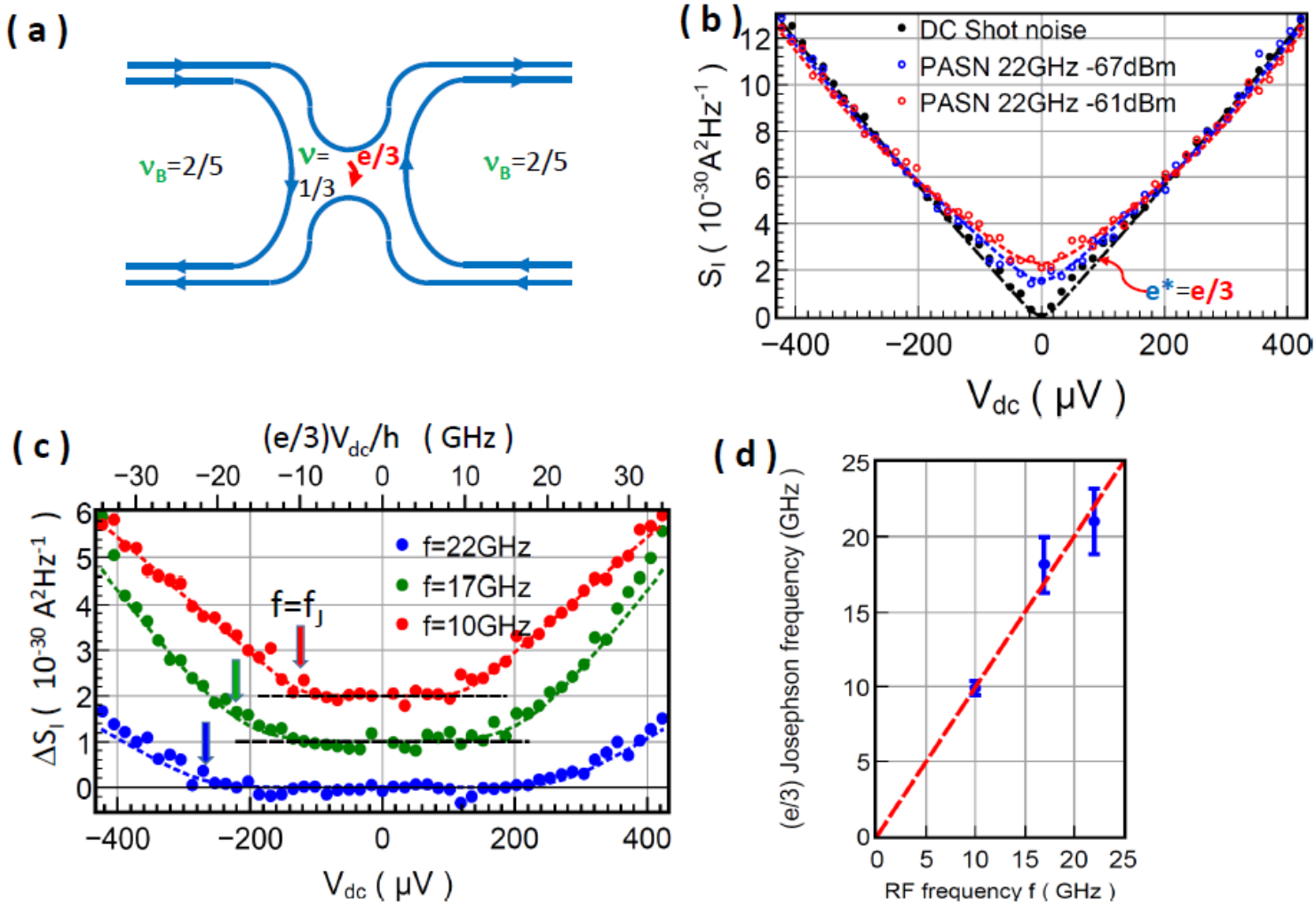
(a)
ν_B=2/5
ν= 1/3
e/3
ν_B=2/5
(b)
DC Shot noise
PASN 22GHz -67dBm
PASN 22GHz -61dBm
S_I (10^{-30} A^2Hz^{-1})
e*=e/3
V_{dc} (μV)
(c)
(e/3)V_{dc}/h (GHz)
f=22GHz
f=17GHz
f=10GHz
f=f_J
ΔS_I (10^{-30} A^2Hz^{-1})
V_{dc} (μV)
(d)
(e/3) Josephson frequency (GHz)
RF frequency f (GHz)

Figure 2

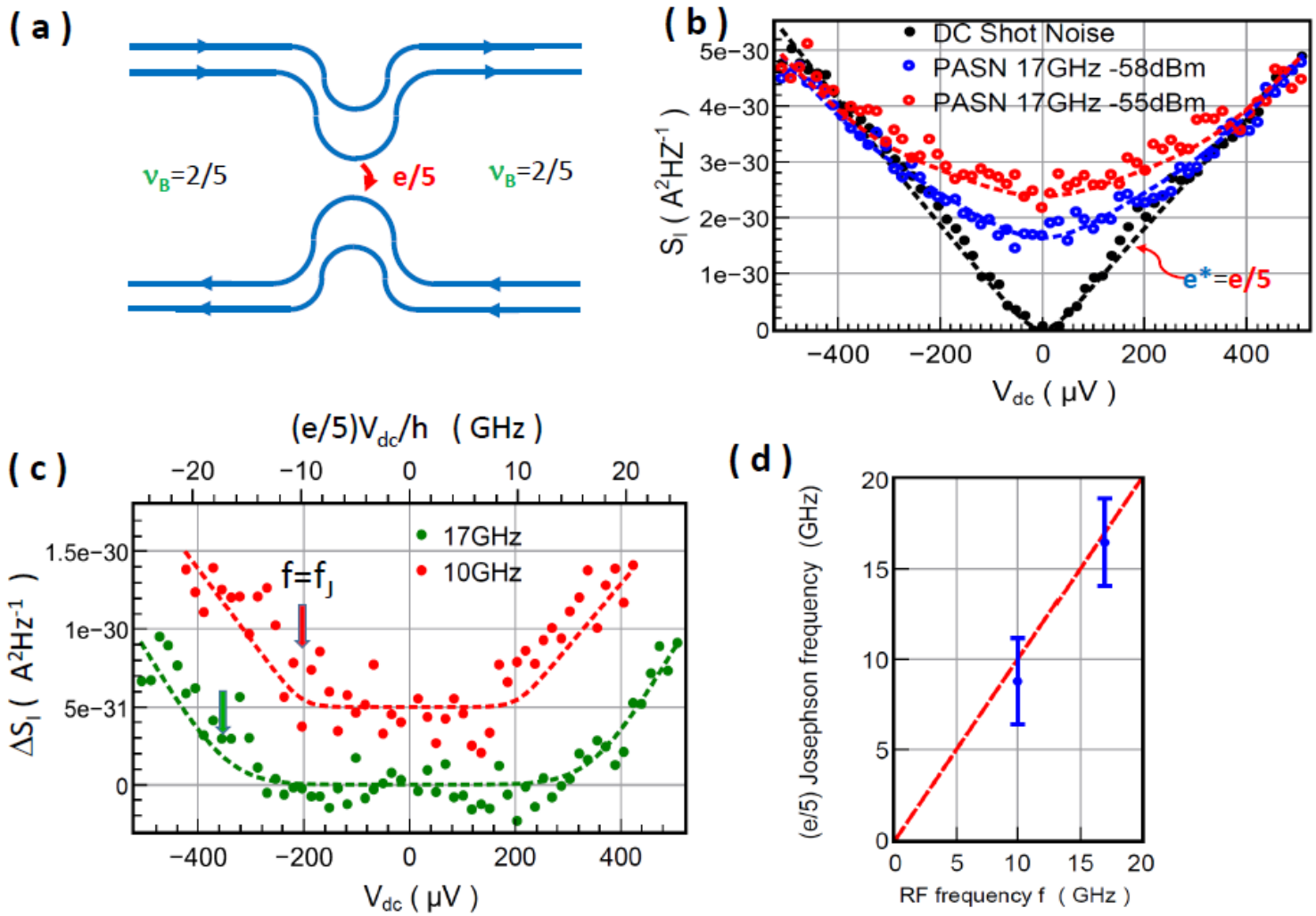
(a)
ν_B=2/5
e/5
ν_B=2/5
(b)
DC Shot Noise
PASN 17GHz -58dBm
PASN 17GHz -55dBm
S_I (A^2HZ^{-1})
5e−30
4e−30
3e−30
2e−30
1e−30
0
−400
−200
0
200
400
V_{dc} (μV)
e*=e/5
(c)
(e/5)V_{dc}/h (GHz)
−20
−10
0
10
20
17GHz
10GHz
f=f_J
ΔS_I (A^2Hz^{-1})
1.5e−30
1e−30
5e−31
0
−400
−200
0
200
400
V_{dc} (μV)
(d)
(e/5) Josephson frequency (GHz)
20
15
10
5
0
0
5
10
15
20
RF frequency f (GHz)

Figure 3

Supplementary Information is available in the online version of the paper.

Acknowledgements We acknowledge the ANR grant FullyQuantum and thank P. Jacques for technical help, P. Pari, P. Forget and M. de Combarieu for cryogenic support, and discussions with I. Safi, Th. Martin, X. Waintal, H. Saleur and members of the Saclay Nanoelectronics Group. DR and IF acknowledge the EPSRC

Author Contributions D.C.G. designed the project. M.K. made the measurements and with P.R. and D.C.G. did the data analysis. All authors discussed the results and contribute to writing the article. Samples were nanolithographied by M.K. on wafers from D.R. and I.F.

Author Information Reprints and permissions information is available at www.nature.com/reprints. The authors declare no competing financial interests. Readers are welcome to comment on the online version of the paper. Correspondence and requests for materials should be addressed to D.C.G. (christian.glattli@cea.fr).